Title

Redox-Responsive Gene Delivery from Perfluorocarbon Nanoemulsions through Cleavable Poly(2-oxazoline) Surfactants

Journal

Angewandte Chemie International Edition, 60(32)

ISSN

1433-7851

Authors

Estabrook, Daniel A
Day, Rachael A
Sletten, Ellen M

Publication Date

2021-08-02

DOI

10.1002/anie.202102413

Peer reviewed

HHS Public Access

Author manuscript

Angew Chem Int Ed Engl. Author manuscript; available in PMC 2022 August 02.

Published in final edited form as:

Angew Chem Int Ed Engl. 2021 August 02; 60(32): 17362–17367. doi:10.1002/anie.202102413.

Redox-responsive gene delivery from perfluorocarbon nanoemulsions through cleavable poly(2-oxazoline) surfactants

Daniel A. Estabrook, **Rachael A. Day**, **Ellen M. Sletten**

Department of Chemistry and Biochemistry, University of California, Los Angeles, 607 Charles E. Young, Dr. E., Los Angeles, CA 90095, USA.

Abstract

The clinical utility of emulsions as delivery vehicles is hindered by a dependence on passive release. Stimuli-responsive emulsions overcome this limitation but rely on external triggers or are composed of nanoparticle-stabilized droplets that preclude sizes necessary for biomedical applications. Here, we employ cleavable poly(2-oxazoline) diblock copolymer surfactants to form perfluorocarbon (PFC) nanoemulsions that release cargo upon exposure to glutathione. These surfactants allow for the first example of redox-responsive nanoemulsions *in cellulo*. A noncovalent fluorous tagging strategy is leveraged to solubilize a GFP plasmid inside the PFC nanoemulsions, whereupon protein expression is achieved selectively when employing a stimuli-responsive surfactant. This work contributes a methodology for non-viral gene delivery and represents a general approach to nanoemulsions that respond to endogenous stimuli.

Graphical Abstract

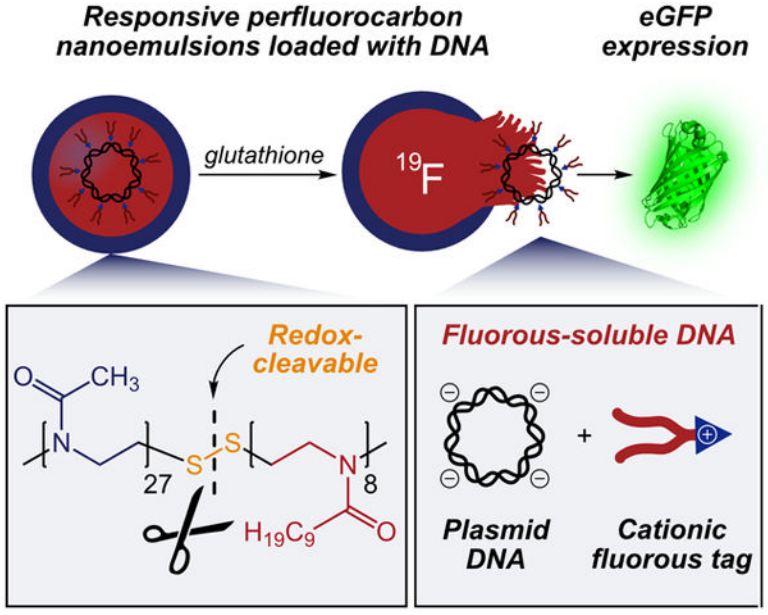

Sletten@chem.ucla.edu.

Supporting information for this article is given via a link at the end of the document.

A disulfide-linked poly(2-oxazoline) surfactant allows for stabilization of perfluorocarbon-in-water nanoemulsions. Upon reduction, the surfactant is cleaved, triggering destabilization and subsequent release of the encapsulated payload. Stimuli-responsive behavior is achieved selectively in high concentrations of reducing agent, allowing for delivery of fluorous-tagged plasmid DNA encoding for enhanced green fluorescent protein.

Keywords

emulsion; gene delivery; stimuli-responsive; interfacial chemistry; poly(2-oxazoline)

Emulsions are among the oldest drug carriers, having been explored since World War II for parenteral delivery.[1] This long-standing interest has yet to wane as 2018 saw over 250 global clinical trials using emulsion systems.[2] In a biomedical context, these liquid-in-liquid droplets benefit from high loading capacity, enhanced bioavailability, and protection of encapsulated cargo from physical and enzymatic degradation.[3,4] Nanoemulsions—droplets less than ~200 nm—are well-suited to biomedical applications due to their small size and long-term kinetic stability.[5] While the former results in extended half-lives *in vivo* and tumor accumulation,[6] the latter allows for stability and tolerance to environmental changes (*e.g.,* pH, temperature).[7] The *in vivo* fate of nanoemulsions is affected by both the interior lipophilic core and surface properties.[8] Despite their clinical utility, currently all five FDA-approved emulsion formulations involve passive release of small molecule payloads (Fig. 1).[2,7] To establish these nanomaterials as site-specific delivery vehicles, payload retention must be controlled by a biological stimulus. Here, we report perfluorocarbon (PFC)-in-water nanoemulsions where passive release is minimized due to the bioorthogonal fluorous phase and stimuli-responsive release is achieved by use of reduction-sensitive amphiphiles.

To date, efforts to deliver payloads from emulsions *in vivo* have centered on the use of ultrasound as a non-invasive exogenous trigger. In these applications, PFC nanoemulsions are chosen due to the ability of PFCs to undergo ultrasound-mediated cavitation, releasing encapsulated cargo (Fig. 1).[9,10] Unfortunately, this behavior is accompanied by off-target effects including tissue and blood vessel damage, as well as the transient perforation of cell membranes.[11] Alternatively, Lanza and Wickline have utilized lipid-coated PFC nanoemulsions for “contact-facilitated drug delivery.”[12] However, this approach is limited to small molecule payloads loaded in the surfactant layer.

Our interest in PFC nanoemulsions stems from the bioorthogonal, nontoxic fluorous core and the ability to sequester fluorous-soluble payloads. This shields cargo from the surrounding environment and minimizes passive release in the presence of cell membrane mimics.[13,14] Certain PFCs have well-documented safety profiles, with FDA-approved applications employing the PFC as a contrast agent and/or oxygen carrier.[15] The main challenge with PFC nanoemulsions as delivery vehicles is solubilizing payloads in the fluorous phase. We have successfully encapsulated small molecule fluorophores and therapeutics within PFC nanoemulsions through covalent attachment of fluorous tags.[14,16–19] Recently, Medina and coworkers extended the payloads capable of being delivered

with PFC nanoemulsions to include proteins by creating a “fluorous mask” around GFP with non-covalent fluorinated anionic tags.[20] GFP was then delivered in cells using ultrasound-induced cavitation. In this manuscript, we further extend the scope of payloads for these vehicles to include DNA using non-covalently associated cationic fluorous tags. Instead of ultrasound-triggered delivery, we control release of the oligonucleotide through a designer surfactant that responds to intracellular concentrations of glutathione.

To obtain a stimuli-responsive surfactant, we envisioned that a cleavable bond could link the hydrophilic and hydrophobic blocks of a diblock copolymer such that, upon stimulus, the surfactant would be irreversibly cleaved. The separated hydrophilic and hydrophobic homopolymers, having no surface activity, would no longer stabilize droplets, leading to demulsification. Previous work on responsive emulsions has involved a variety of stimuli, including pH[21–23], ions[24], gases[25,26], temperature[27,28], and redox agents[29,30]. Among these, redox agents are appealing for intracellular delivery vehicles due to the high concentration of reducing agents within the cell. Redox-responsive surfactants have been reported that contain functionalities such as ferrocenes[31,32], selenium atoms[29,33], and disulfide bonds[30,34,35]. However, these surfactants were not explored as emulsifiers for nanoemulsions.

We have previously developed poly(2-oxazoline) (POx) block copolymer surfactants capable of stabilizing oil-in-water nanoemulsions.[18,19] These amphiphiles form sub-200 nm droplets through emulsification involving either PFCs or olive oil as the emulsion core. We found that a poly(2-methyl-2-oxazoline)-*b*-poly(2-nonyl-2-oxazoline) ($P(MeOx)_{30}$-*b*-$P(NonOx)_{12}$, **6**, Fig. 2A) diblock copolymer was optimal for emulsions of <200 nm size with stability over 60 days. Building from this, we designed a reduction-sensitive surfactant with a disulfide bond linking the $P(MeOx)_{30}$ and $P(NonOx)_{10}$ blocks (**5**, Fig. 2A). Hydrophilic and hydrophobic homopolymers of $P(MeOx)_{30}$ and $P(NonOx)_{10}$ were synthesized through polymerization of their monomers (**1** and **3**) and terminated with potassium thioacetate.[36,37] To bias disulfide exchange, $P(MeOx)_{24}$-*t*-SAc was reacted with Aldrithiol to yield $P(MeOx)_{27}$-*t*-SS-Pyr, **4**.[36,38] End-group fidelity was confirmed by ^{1}H-NMR and MALDI-TOF analysis (see Table 1 and ESI). Polymer-polymer coupling was performed via *in situ* deprotection and disulfide exchange between $P(NonOx)_{10}$-*t*-SAc, **2** (1.0 equiv.), and **4** (1.2 equiv.) to yield disulfide-linked $P(MeOx)_{27}$-SS-$P(NonOx)_8$, **5** (Fig. 2A). While homopolymer coupling was a concern, MALDI-TOF demonstrated that these byproducts were minimal and mass patterns in responsive surfactant **5** resembled control surfactant **6** (Fig. 2C, Fig. S1–S2).

With a responsive surfactant in hand, we confirmed that **5** stabilized PFC-in-water nanoemulsions with a size distribution similar to our previously reported non-responsive **6**.[18] To form PFC nanoemulsions, polymers **5** or **6** were solubilized in dimethylformamide and diluted with phosphate buffered saline (PBS, pH 7.4) to a surfactant loading of 15 wt%. This solution was then ultrasonicated alongside 10 vol% PFC (Fig. 2B). Dynamic light scattering analysis of the resulting PFC nanoemulsions showed similar size distributions, with **5** and **6** stabilizing droplets of 200 nm and 180 nm, respectively (Fig. 2D, Fig. S3–S4).[39] When employed for olive oil nanoemulsions, **5** and **6** resulted in droplets of 170 nm and 140 nm, respectively (Fig. S5–S6).

Next, we characterized the responsive nature of the droplets. We envisioned that the disulfide would be located at the liquid-liquid interface due to positioning between the hydrophilic and hydrophobic blocks and could be accessed with reducing agent. Thus, disulfide reduction would lead to destruction of the surfactant, destabilization of the droplet, and release of encapsulated cargo (Fig. 3A). Glutathione (GSH) was chosen as the stimulus as it is present at concentrations 100 to 1000 times higher in the cytosol (~10 mM) than within extracellular fluids (~0.1 mM).[40] First, we compared release behavior of **5**- or **6**-stabilized PFC droplets to GSH on the macroscale using fluorescein to track the aqueous phase and a fluorous-soluble rhodamine dye (**8**, Fig. 3b)[34] to track the fluorous phase (Fig. 3C, i). Surfactants **5** and **6** were added to each layer (2.8 wt%), and emulsified (Fig. 3C, ii). GSH was then added at cytosolic concentrations (10 mM). After three hours, demulsification and phase separation were observed with surfactant **5**. Gratifyingly, non-responsive surfactant **6** showed no change (Fig. 3C, iii, Fig. S7). Turbidity of emulsion solutions in the presence of 0, 0.1, 1 and 10 mM GSH was characterized, indicating that vehicles were stable from 0–1 mM GSH (Fig. S8). We confirmed that demulsification was a result of amphiphile cleavage through MALDI-TOF analysis of responsive surfactant **5** after exposure to GSH (Fig. S9–S10). Only trace amounts of $P(MeOx)_x$-SS-$P(NonOx)_y$ products were observed after treatment with 10 mM GSH, with the major products being thiol-capped homopolymers (**9**, **10,** Fig. 3A), or residual disulfide-linked $P(NonOx)_x$-SS-$P(NonOx)_y$ (Fig S10). We hypothesized that the hydrophobic environment hindered reduction by hydrophilic GSH.[41] Collectively, these data indicate that the disulfide is critical to demulsifying redox-responsive nanoemulsions in response to a biological trigger.

Having confirmed that responsive amphiphiles can induce demulsification, we examined payload release kinetics. We again employed **8** as a payload and assayed release from nanoemulsions stabilized by **5** or **6** at no (0 mM), low (extracellular, 0.1 mM) or high (intracellular, 10 mM) levels of GSH. Emulsions were partitioned against 1-octanol, a lipid bilayer mimic (Fig. 3D).

Photoluminescence of the 1-octanol was monitored over 72 hours to determine payload leaching (Fig. 3E). As expected, control surfactant **6** showed payload stability over varying concentrations of GSH (Fig. S11 for inset between 0–10 au). Conversely, stimuli-responsive surfactant **5** demonstrated dose-response to GSH. No and low (0.1 mM) concentrations of GSH resulted in little leaching while exposure to high (10 mM) GSH resulted in a sustained release profile. Other experiments investigating release of **8** under multi-fold concentrations of GSH (0, 1, 0.1 and 10 mM) at physiological temperature (37 °C) demonstrated dose-dependent release in response to reducing concentrations (Fig. S12). Additionally, release was analyzed under 5000-fold dilution by dialyzing **5**- and **6**-stabilized PFC nanoemulsions containing **8** in either PBS or GSH (10 mM) overnight (Fig. S13). While control **6** showed payload stability with and without GSH, cleavable surfactant **5** achieved quantitative release only in GSH. The mechanism of demulsification and subsequent release was further probed, suggesting that at dilute conditions relevant to cellular delivery, destruction of the block copolymer reduces the kinetic barrier to releasing the encapsulated payload, thus delivering it to the surrounding environment (Fig. S14–S17, SI Note 1). Finally, we probed the stability of a panel of fluorous-soluble fluorophores[13,14,42] in **6**-stabilized droplets in the presence

of albumin at physiological conditions (Fig. S18–S20), demonstrating that albumin plays a minimal role in the leaching of fluorous payloads from the nanoemulsions.

After demonstrating responsive PFC nanoemulsions *in vitro*, we extended use to *in cellulo* DNA delivery. Efforts within gene delivery using polymeric materials, *e.g.,* polyethyleneimine (PEI) are often limited by inefficient gene release.[43] Nucleic acid delivery with oil nanoemulsions has been explored since the mid-90s, with the major loading strategy being electrostatic adsorption of cationic surfactants with the phosphodiester backbone.[44] More recently, plasmid encapsulation in a hydrocarbon oil core was reported and compared to surface adsorption loading methods.[45] While adsorption suffered from burst release behavior, encapsulation suffered the inverse—plasmid was not released even after 48 h of media incubation. Herein, we demonstrate the ability to selectively release pDNA from a bioorthogonal fluorinated liquid core and drive protein expression *in cellulo*, representing an avenue for nonviral gene delivery. This first required a strategy to solubilize hydrophilic DNA into the non-polarizable fluorous phase. Fundamental studies by Bühlmann and coworkers have quantified ion pairs to be ~10^5 times stronger in fluorous solvents than organic solvents,[46] suggesting electrostatic interactions between the anionic backbone of DNA and a cationic fluorous tag would be a fruitful approach to loading PFC nanoemulsions with DNA.

We employed ammonium **11** with two C_6F_{13} chains[42] as a fluorous tag to solubilize plasmid (pDNA) in perfluorocarbon (Fig. 4A). Importantly, this tag is designed to maximize fluorous solubility while retaining biocompatible perfluorocarbon segments.[47] For the pDNA, we chose an eGFP plasmid such that a fluorescence readout could measure payload delivery. Notably, cytosolic delivery and nuclear entry of the pDNA are essential for gene expression (Fig. 4B). We combined **11** (7.7 mg) with eGFP pDNA (5, 15 or 30 μg) and freeze-dried overnight. The pDNA/**11** polyplex was then dissolved in a PFC mixture and sonicated (Fig. 4A). Model poly(2-oxazoline) amphiphile poly(2-ethyl-2-oxazoline)$_{90}$-*b*-poly(2-nonyl-2-oxazoline)$_{10}$ [19] was solubilized in dimethylformamide and diluted with PBS (pH 7.4) to a loading of 2.8 wt%. This solution was combined with 10 vol% of the PFC/pDNA/**11** mixture and ultrasonicated. To verify encapsulation, supernatant was separated and solution corresponding to eGFP loaded within PFC nanoemulsions was analyzed on an agarose gel (Fig. 4C). DNA bands were assigned following literature precedent.[48] These data showed that eGFP pDNA could be loaded into PFC droplets in a dose-dependent manner from 5–30 μg. By comparison, electrophoresis of the supernatant solution showed reduced pDNA (Fig. S21). These data were verified by fluorescence experiments using Thiazole Orange, a DNA-binding dye suggesting that 40 ± 4% of the pDNA was encapsulated in the 30 μg sample (Fig. S22).

With the **11**/pDNA complex loaded into PFC nanoemulsions, we investigated the ability of responsive surfactant **5** to promote eGFP expression (Fig. 4B). Emulsion formation was accomplished with responsive surfactant **5** or control surfactant **6**. We also combined homopolymers **2** and **4** with perfluorocarbon containing **11**/pDNA complex, yielding heterogenous aggregates (Fig. S23), to control for the role of the homopolymers. To monitor transfection efficiency, eGFP pDNA complexed with lipofectamine was added as a positive control. Human embryonic kidney cells (HEK-293) were treated with pDNA-loaded

nanomaterials for 3 hours in media (+10% FBS). Non-uptaken emulsions were then washed away and cells were incubated in the presence or absence of GSH (10 mM) overnight.[49,50] The following day, cells were washed and analyzed by flow cytometry (Fig. 4D). Incubation with control **6**-stabilized droplets or a combination of homopolymers **2** and **4** resulted in statistically insignificant expression regardless of GSH treatment. By contrast, responsive **5**-stabilized emulsions showed effective eGFP expression only in cells treated with GSH buffer, while untreated cells had fluorescence similar to that of control **6**. These data suggest that the cleavable disulfide within **5**-stabilized droplets enables release of encapsulated eGFP pDNA. While we cannot completely rule out that residual PFC nanoemulsions or prematurely released pDNA persisted extracellularly after washing, control experiments with **11**/pDNA either free or alongside homopolymers **2** and **4** suggest that these scenarios would not lead to eGFP expression, giving us confidence that cleavage occurs intracellularly. Finally, treating cells with endosomal escape agent chloroquine had no benefit over treatments with GSH buffer alone (Fig. S26).

In summary, we have demonstrated the use of disulfide-linked poly(2-oxazoline) amphiphiles as stimuli-responsive surfactants for nanoemulsions. Reduction of the disulfide linkage results in destabilization of the PFC-in-water nanoemulsions and release of an encapsulated payload. While we did find that buffering cells with GSH was required to achieve adequate transfection, we envision further tuning of the reactivity-stability balance of the nanoemulsions will enable more rapid response without the need for additional GSH. Furthermore, the concept of cleavable amphiphilic surfactants presented herein can readily be extended to other endogenous stimuli such as changes in pH or reactive oxygen species. The former is potentially advantageous as endosomal escape of the nanoemulsions will not be required for delivery[51], while the latter is particularly conducive to use with PFC nanoemulsions that have high oxygen content[52]. Alongside the new approach to stimuli-responsive nanoemulsions, we present a fluorous tag strategy to solubilize a nucleic acid—plasmid DNA—within a fluorinated liquid core. Combining these advances, we show that eGFP expression is controlled by use of the responsive delivery vehicle. Overall, these cleavable polymeric amphiphiles demonstrate that macroscale behavior of droplets can be dictated by block copolymer design and are poised to expand applications of emulsions in drug delivery.

Supplementary Material

Refer to Web version on PubMed Central for supplementary material.

Acknowledgements

Funding was provided by the following grants to E.M.S.: University of California Cancer Research Coordinating Committee (CNR-18–524809), American Chemical Society Petroleum Research Fund (57379-DNI4), Alfred P. Sloan Award (FG-2018–10855), and Hellman Fellows Award. D.A.E. was supported by T32 training grants from the National Institutes of Health (5T32GM067555–12), the Dissertation Year Fellowship, and the Majeti-Alapati Fellowship. R.A.D. was supported by the Saul Winstein Fellowship. NMR data were obtained on instruments funded by the National Science Foundation (MRI CHE-1048804). We thank Heidi van de Wouw and Margeaux A. Miller for synthesis of **11**. We thank Chris G. Jones for help with statistical analysis.

References

[1]. Collins-Gold LC, Lyons RT, Bartholow LC, Adv. Drug Deliv. Rev 1990, 5, 189–208.

[2]. Zhong H, Chan G, Hu Y, Hu H, Ouyang D, Pharmaceutics 2018, 10, 263.

[3]. Chime SA, Kenechukwu FC, Attama AA, in Appl. Nanotechnol. Drug Deliv, 2014.

[4]. Pathak K, Pattnaik S, Swain K, in Nanoemulsions Formul. Appl. Charact, 2018, pp. 415–433.

[5]. Mason TG, Wilking JN, Meleson K, Chang CB, Graves SM, J. Phys. Condens. Matter 2006, 18, R635–R666.

[6]. Nel A, Ruoslahti E, Meng H, ACS Nano 2017, 11, 9567–9569. [PubMed: 29065443]

[7]. Singh Y, Meher JG, Raval K, Khan FA, Chaurasia M, Jain NK, Chourasia MK, Control J. Release 2017, 252, 28–49.

[8]. Ganta S, Talekar M, Singh A, Coleman TP, Amiji MM, AAPS PharmSciTech 2014, 15, 694–708. [PubMed: 24510526]

[9]. Rapoport N, Wiley Interdiscip. Rev. Nanomedicine Nanobiotechnology 2012, 4, 492–510. [PubMed: 22730185]

[10]. Kripfgans OD, Fowlkes JB, Miller DL, Eldevik OP, Carson PL, Ultrasound Med. Biol 2000, 26, 1177–1189. [PubMed: 11053753]

[11]. Rapoport N, Gao Z, Kennedy A, Natl J. Cancer Inst 2007, 99, 1095–1106.

[12]. Winter PM, Cai K, Caruthers SD, Wickline SA, Lanza GM, Expert Rev. Med. Devices 2007, 4, 137–145. [PubMed: 17359221]

[13]. Sletten EM, Swager TM, J. Am. Chem. Soc 2014, 136, 13574–13577. [PubMed: 25229987]

[14]. Lim I, Vian A, Van De Wouw HL, Day RA, Gomez C, Liu Y, Rheingold AL, Campàs O, Sletten EM, J. Am. Chem. Soc 2020, 142, 16072–16081.

[15]. Riess JG, Artif. Cells. Blood Substit. Immobil. Biotechnol 2005, 33, 47–63. [PubMed: 15768565]

[16]. Miller MA, Day RA, Estabrook DA, Sletten EM, Synlett 2020, 31, 450–454.

[17]. Day RA, Estabrook DA, Logan JK, Sletten EM, Chem. Commun 2017, 53, 13043–13046.

[18]. Estabrook DA, Ennis AF, Day RA, Sletten EM, Chem. Sci 2019, 10, 3994–4003. [PubMed: 31015940]

[19]. Day RA, Estabrook DA, Wu C, Chapman JO, Togle AJ, Sletten EM, ACS Appl. Mater. Interfaces 2020, 12, 38887–38898. [PubMed: 32706233]

[20]. Sloand JN, Nguyen TT, Zinck SA, Cook EC, Zimudzi TJ, Showalter SA, Glick AB, Simon JC, Medina SH, ACS Nano 2020, 14, 4061–4073. [PubMed: 32134630]

[21]. Fujii S, Cai Y, Weaver JVM, Armes SP, J. Am. Chem. Soc 2005, 127, 7304–7305. [PubMed: 15898766]

[22]. Tu F, Lee D, J. Am. Chem. Soc 2014, 136, 9999–10006. [PubMed: 24791976]

[23]. Liu K, Jiang J, Cui Z, Binks BP, Langmuir 2017, 33, 2296–2305. [PubMed: 28191963]

[24]. Binks BP, Rodrigues JA, Angew. Chem. Int. Ed 2005, 44, 441–444.

[25]. Liu Y, Jessop PG, Cunningham M, Eckert CA, Liotta CL, Science 2006, 313, 958–960. [PubMed: 16917059]

[26]. Jiang J, Zhu Y, Cui Z, Binks BP, Angew. Chem. Int. Ed 2013, 52, 12373–12376.

[27]. Binks BP, Murakami R, Armes SP, Fujii S, Angew. Chem. Int. Ed 2005, 44, 4795–4798.

[28]. Wiese S, Spiess AC, Richtering W, Angew. Chem. Int. Ed 2013, 52, 576–579.

[29]. Kong W, Guo S, Wu S, Liu X, Zhang Y, Langmuir 2016, 32, 9846–9853. [PubMed: 27595739]

[30]. Sivakumar S, Bansal V, Cortez C, Chong SF, Zelikin AN, Caruso F, Adv. Mater 2009, 21, 1820–1824.

[31]. Aydogan N, Abbott NL, Langmuir 2001, 17, 5703–5706.

[32]. Tsuchiya K, Orihara Y, Kondo Y, Yoshino N, Ohkubo T, Sakai H, Abet M, J. Am. Chem. Soc 2004, 126, 12282–12283. [PubMed: 15453758]

[33]. Zhang Y, Chen H, Liu X, Zhang Y, Fang Y, Qin Z, Langmuir 2016, 32, 13728–13735. [PubMed: 27958741]

[34]. Jong LI, Abbott NL, Langmuir 2000, 16, 5553–5561.

[35]. Deng Z, Yuan S, Xu RX, Liang H, Liu S, Angew. Chem. Int. Ed 2018, 57, 8896–8900.

[36]. Hsiue GH, Chiang HZ, Wang CH, Juang TM, Bioconjug. Chem 2006, 17, 781–786. [PubMed: 16704218]

[37]. Hoogenboom R, Wiesbrock F, Huang H, Leenen MAM, Thijs HML, Van Nispen SFGM, Van Der Loop M, Fustin CA, Jonas AM, Gohy JF, et al., Macromolecules 2006, 39, 4719–4725.

[38]. Velluto D, Thomas SN, Simeoni E, Swartz MA, Hubbell JA, Biomaterials 2011, 32, 9839–9847. [PubMed: 21924769]

[39]. We attributed slight changes in size to be a result of minor P(MeOx)n impurities within 5 that effectively reduced surfactant loading.

[40]. Cheng R, Feng F, Meng F, Deng C, Feijen J, Zhong Z, Control J. Release 2011, 152, 2–12.

[41]. A similar observation was previously noted in the redox reaction of selenium-containing surfactants with H_2O_2, described as “generally time-consuming… [Partially due to the] hydrophobic environment where selenium atoms are located, which is unfavorable for coming into contact with hydrophilic H_2O_2.” [29]

[42]. Miller MA, Sletten EM, Org. Lett 2018, 20, 6850–6854. [PubMed: 30354161]

[43]. Grigsby CL, Leong KW, Soc JR. Interface 2010, 7, S67–S82. [PubMed: 19734186]

[44]. Teixeira HF, Bruxel F, Fraga M, Schuh RS, Zorzi GK, Matte U, Fattal E, Int. J. Pharm 2017, 534, 356–367. [PubMed: 29038065]

[45]. Fraga M, Bruxel F, Diel D, De Carvalho TG, Perez CA, Magalhães-Paniago R, Malachias Â, Oliveira MC, Matte U, Teixeira HF, Control J. Release 2015, 209, 37–46.

[46]. Boswell PG, Bühlmann P, J. Am. Chem. Soc 2005, 127, 8958–8959. [PubMed: 15969566]

[47]. Krafft MP, Riess JG, Curr. Opin. Colloid Interface Sci 2015, 20, 192–212.

[48]. Ando S, Putnam D, Pack DW, Langer R, J. Pharm. Sci 1999, 88, 126–130. [PubMed: 9874713]

[49]. Koo AN, Lee HJ, Kim SE, Chang JH, Park C, Kim C, Park JH, Lee SC, Chem. Commun 2008, 6570–6572.

[50]. Tang LY, Wang YC, Li Y, Du JZ, Wang J, Bioconjug. Chem 2009, 20, 1095–1099. [PubMed: 19438224]

[51]. Gao W, Chan JM, Farokhzad OC, Mol. Pharm 2010, 7, 1913–1920. [PubMed: 20836539]

[52]. Day RA, Sletten EM, Curr. Opin. Colloids Inter. Sci. 2021, DOI: 10.1016/j.cocis.2021.101454.

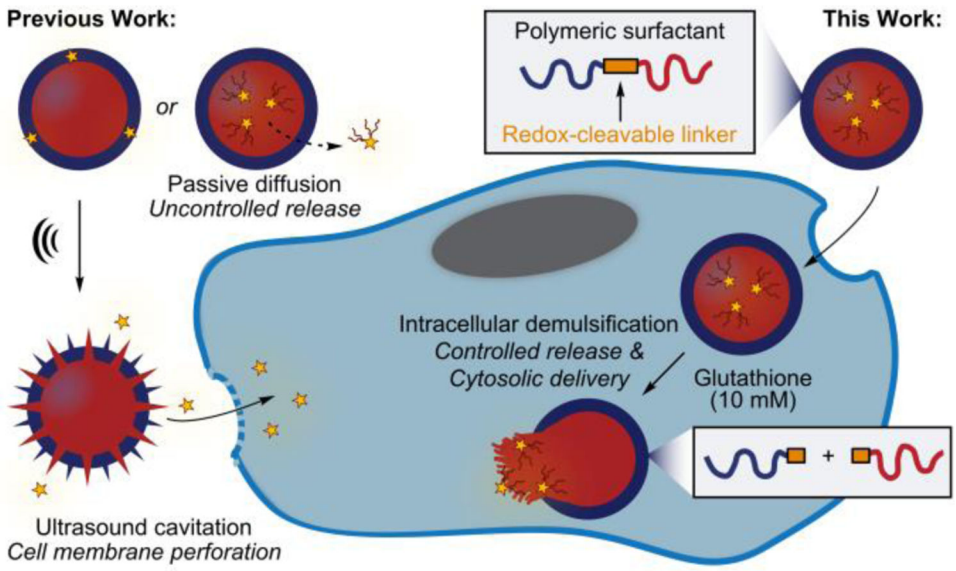

Figure 1.

Traditional methods to control payload release from nanoemulsions are dominated by passive diffusion or ultrasound-induced cavitation (left). In this work, we employ a disulfide-containing block copolymer surfactant to stabilize oil-in-water nanoemulsions. Reduction of the cleavable surfactant triggers demulsification and release of encapsulated cargo (right).

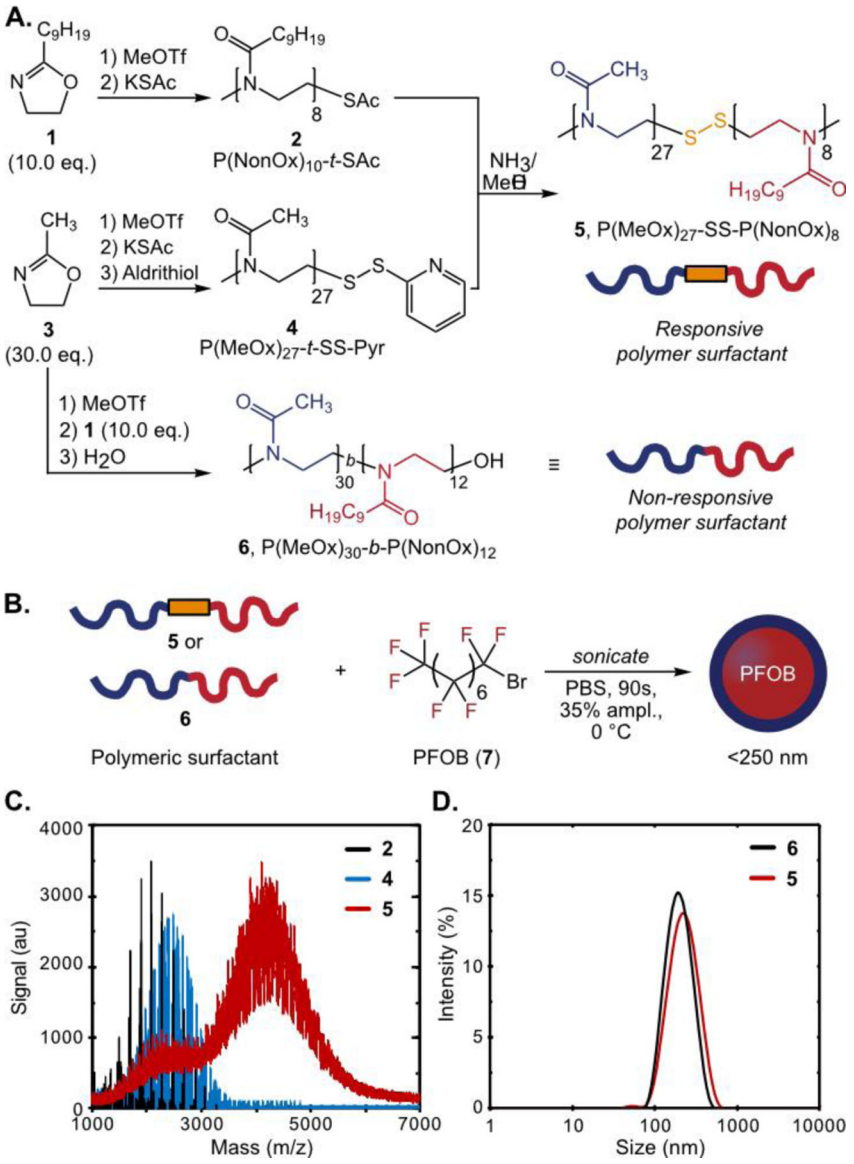

Figure 2.

Synthesis and characterization of diblock copolymers and their use as surfactants for PFC-in-water nanoemulsions. (A) Synthesis of responsive copolymer **5** and control polymer **6**.[18] (B) Surfactants **5** or **6** stabilize perfluorooctylbromide (**7**, PFOB) nanoemulsions. (C) MALDI-TOF of **2**, **4** and **5**. (D) Dynamic light scattering of PFC nanoemulsions stabilized by **5** or **6**. Data are an average of three replicate measurements. See Fig. S3, S4 for intensity and number % traces.

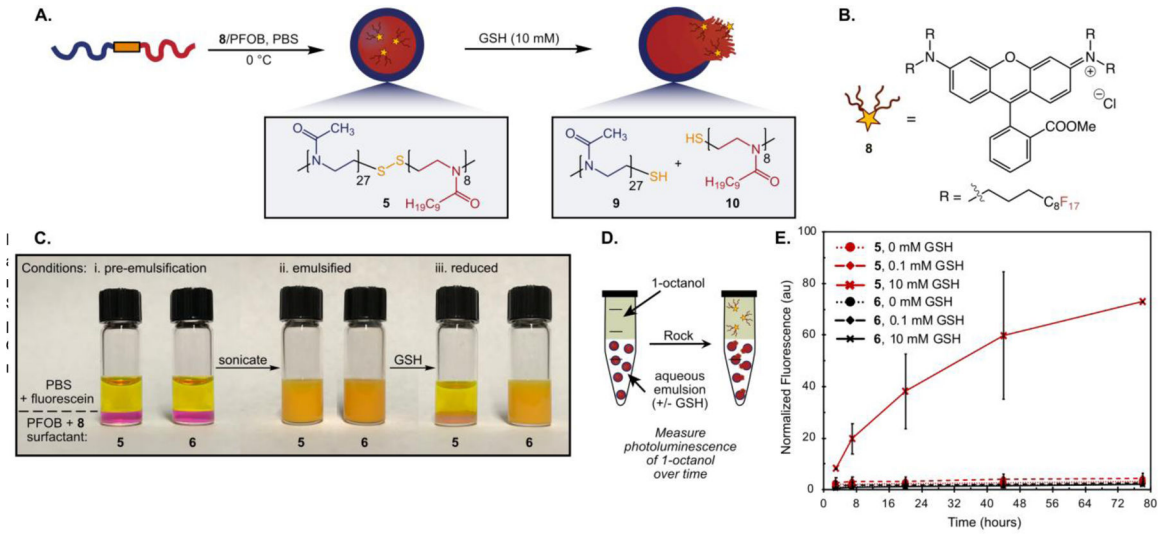

Figure 3.

Responsive surfactants allow for demulsification and payload release in the presence of reducing agent. (A) Responsive PFC nanoemulsions from amphiphile **5**. When exposed to GSH (10 mM), the disulfide is reduced resulting in homopolymers **9** and **10**, facilitating payload release. (B) Model payload, rhodamine **8**. (C) (i) Solutions of fluorescein (3.0 mM), **5** or **6** (1.7 wt%) solubilized in PBS (pH 7.4) and combined with **8** solubilized in PFOB (0.13 mM). (ii) Solutions in (i) after sonication. (iii) Emulsions in (ii) treated with GSH (10 mM) and rocked (25 °C, 3 h). (D) Schematic of partition experiment to determine payload leaching, modeled by **8**. (D) Nanoemulsions stabilized by **5** or **6** were prepared containing **8**, diluted 15-fold in PBS with varying concentrations of GSH, combined with 1-octanol, and agitated. The fluorescence of 1-octanol (Ex. 500) was measured over time. Fluorescence was normalized to **6**-stabilized nanoemulsions at 3 h without GSH. Error bars represent the standard deviation of two independent experiments. See Fig. S11 for insert between 0–10 au.

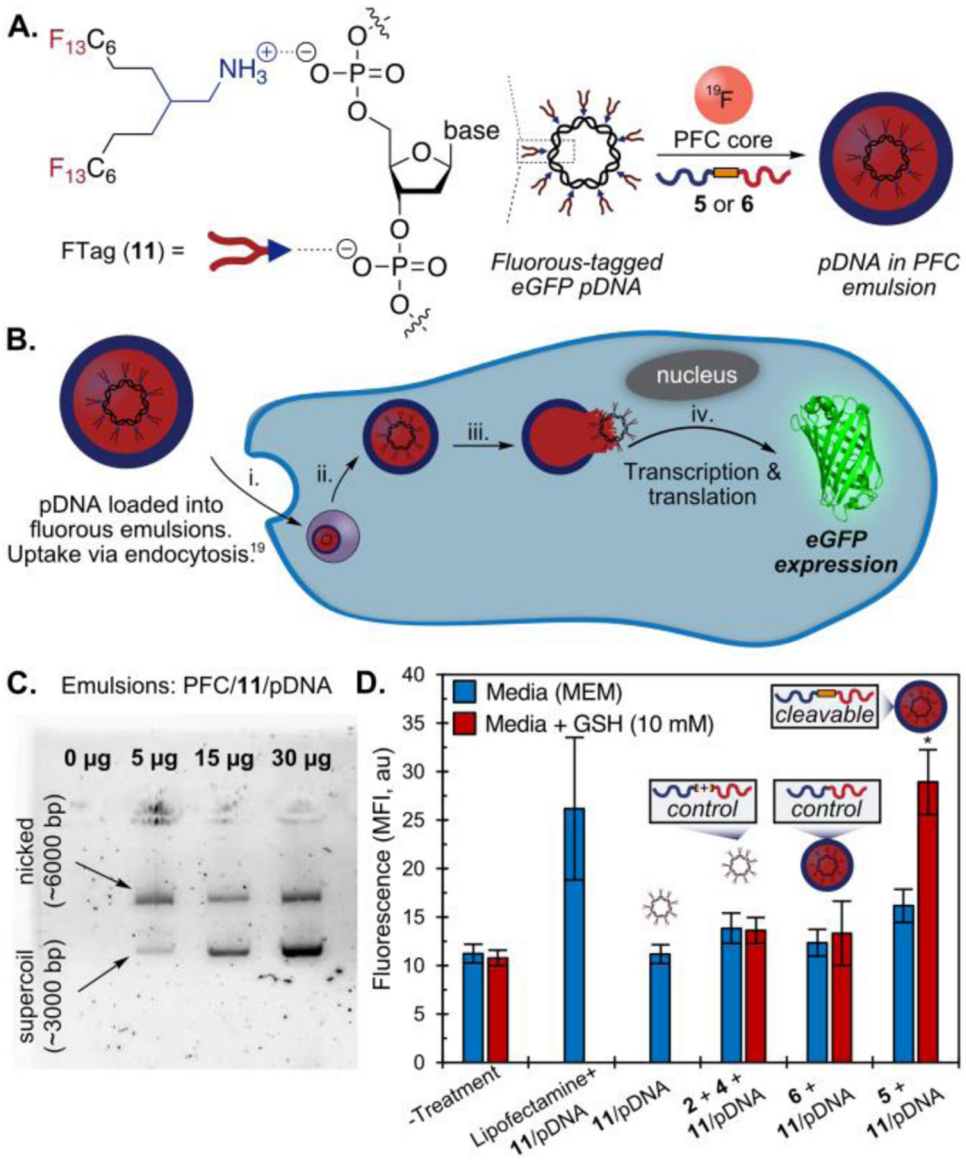

Figure 4.

Delivery of eGFP pDNA with GSH-responsive nanoemulsions. (A) Fluorous amine tag (**11**) complexes with eGFP pDNA, solubilizing it within a PFC core that is sonicated in the presence of **5** or **6** to form **11**/eGFP PFC nanoemulsions. (B) Schematic of delivery and eGFP expression. (C) Gel electrophoresis of destroyed PFC emulsions loaded with different amounts of pDNA complexed with **11**. (D) Flow cytometry of HEK-293 cells incubated with PFC/**11**/pDNA nanoemulsions for 3 hours in MEM media (+ 10% FBS). Cells were washed and incubated with MEM media with or without GSH (10 mM) overnight. Cells were trypsonized, washed, resuspended in FACS buffer and analyzed for eGFP fluorescence by flow cytometry. Data is representative of three independent experiments. See Fig. S24–S26 for histograms of independent experiments. Statistical significance is defined by ANOVA

test followed by Tukey HSD test for significance. α is defined as 0.05. See Fig. S27 for analysis.

Author Manuscript

Author Manuscript

Author Manuscript

Table 1.

Characterization of polymers **2**, **4**–**6**.

#	Polymer	M_w (kDa)	M_n (kDa)	$Đ$
2[a]	P(NonOx)$_{10}$-*t*-SAc	2.4	2.1	1.11
4[a]	P(MeOx)$_{27}$-*t*-SS-Pyr	2.4	2.3	1.06
5[a]	P(MeOx)$_{27}$-SS-P(NonOx)$_8$	4.2	3.8	1.09
6[b]	P(MeOx)$_{30}$-*b*-P(NonOx)$_{12}$	5.1	4.8	1.24

[a]Characterized by MALDI.

[b]Characterized as previously reported.[18]